

Cohesive Crack Analysis of Toughness Increase Due to Confining Pressure

KAZUSHI SATO,¹ and TOSHIYUKI HASHIDA²

Abstract:—Apparent fracture toughness in Mode I of microcracking materials such as rocks under confining pressure is analyzed based on a cohesive crack model. In rocks, the apparent fracture toughness for crack propagation varies with the confining pressure. This study provides analytical solutions for the apparent fracture toughness using a cohesive crack model, which is a model for the fracture process zone. The problem analyzed in this study is a fluid-driven fracture of a two-dimensional crack with a cohesive zone under confining pressure. The size of the cohesive zone is assumed to be negligibly small in comparison to the crack length. The analyses are performed for two types of cohesive stress distribution, namely the constant cohesive stress (Dugdale model) and the linearly decreasing cohesive stress. Furthermore, the problem for a more general cohesive stress distribution is analyzed based on the fracture energy concept. The analytical solutions are confirmed by comparing them with the results of numerical computations performed using the body force method. The analytical solution suggests a substantial increase in the apparent fracture toughness due to increased confining pressures, even if the size of the fracture process zone is small.

Key words: Rock, fracture toughness, cohesive crack model, confining pressure, stress intensity factor.

1. Introduction

It has been reported that fracture toughness of rocks increases with increasing confining pressure (SCHMIDT and HUDDLE, 1977; ABOU-SAYED, 1978; FUNATSU *et al.*, 2004). Fracture toughness is often expressed in terms of the stress intensity factor required for crack propagation. In the fracture of a linear elastic solid, the fracture toughness is assumed to be an inherent material property and independent of loading configurations. In rocks, however, the stress intensity factor for crack propagation varies with confining pressure. Therefore, the fracture toughness of rocks should be viewed as an apparent material property.

¹Miyagi National College of Technology, 48 Aza–Nodayama, Shiote, Medeshima, Natori, 981–1239, Japan. E-mail: kazushi@miyagi-ct.ac.jp

²Fracture and Reliability Research Institute, Tohoku University, 01 Aoba, Aramaki, Aoba-ku, Sendai, 980–8579, Japan.

It is well known that the fracture process zone that is formed prior to crack growth is significantly large in size compared to the specimen dimensions for many rock types (LABUZ *et al.*, 1987). Therefore, a suitable model for the fracture process zone is necessary to evaluate the crack growth on the basis of laboratory experiments. A Barenblatt-type cohesive crack model has been applied to express the formation of the fracture process zone in rocks (HASHIDA, 1990; SATO *et al.*, 1995). HASHIDA *et al.* (1993) have reported that the crack growth behavior of Iitate granite under confining pressure up to 26.5 MPa can be predicted using the cohesive crack model (tension-softening model). In the tension-softening model, the fracture process zone is represented as a crack subjected to a cohesive stress which depends on the crack opening displacement. The relation between the cohesive stress and the crack opening displacement is referred to as the tension-softening curve. The critical fracture energy is provided by the area under the tension-softening curve (HILLERBORG, 1983). HASHIDA *et al.* (1993) have concluded that the tension-softening curve is independent of confining pressure. Therefore, it can be seen that the tension-softening curve is the inherent material property to be used to evaluate the crack growth under confining pressure. The cohesive crack model is expected to provide a useful tool for predicting the apparent fracture toughness.

In this study, the apparent fracture toughness under confining pressure is examined using a cohesive crack model. A two-dimensional fluid-driven fracture with cohesive zone under confining pressure is analyzed. Two types of cohesive stress distributions are studied. The size of cohesive zone is assumed to be negligibly small. The apparent fracture toughness is measured in terms of the stress intensity factor induced by the fluid pressure. The theoretical model is verified by comparing it with numerical results obtained by the body force method.

2. Problem Formulation

The problem to be analyzed is a fluid-driven fracture of a two-dimensional crack with cohesive zones under confining pressure in an infinite body, as shown in Figure. 1. Tension is taken to be positive. The plane strain condition is assumed.

The fracture process zone is represented by the cohesive zone. The cohesive zone length is R . The fluid pressure P is applied to the crack surface except within the cohesive zone. The pressurized crack length is $2a$, and the total crack length including the cohesive zone is $2c$. The cracked body is subjected to the confining pressure S at a far distance.

Two types of cohesive stress distributions were analyzed, as shown in Figure. 2. Case 1 represents a model of constant cohesive stress, while case 2 corresponds to a linearly decreasing stress model.

When the fracture process zone is negligibly small, the critical stress intensity factor K_c for the case of constant cohesive stress is

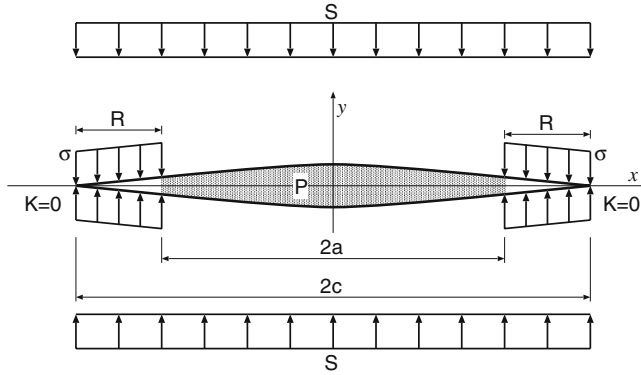


Figure 1

Fluid-driven crack with cohesive zone under confining stress.

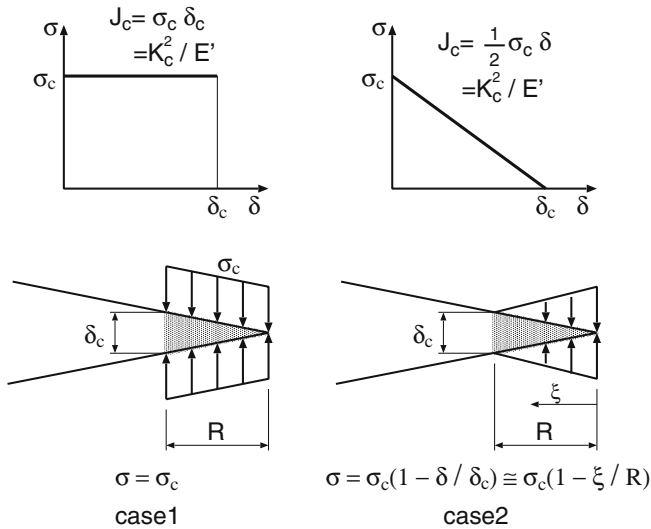


Figure 2

Cohesive stress distributions analyzed in this study: (a) constant cohesive stress and (b) linearly decreasing stress. The cohesive zone length is determined by the critical crack opening displacement δ_c .

$$\frac{K_c^2}{E'} = \sigma_c \delta_c, \tag{1}$$

where σ_c is the peak stress of the cohesive stress, δ_c is the critical crack opening displacement and E' is the effective Young's modulus. For the case of linearly decreasing stress, the critical stress intensity factor is given by

$$\frac{K_c^2}{E'} = \frac{1}{2} \sigma_c \delta_c. \tag{2}$$

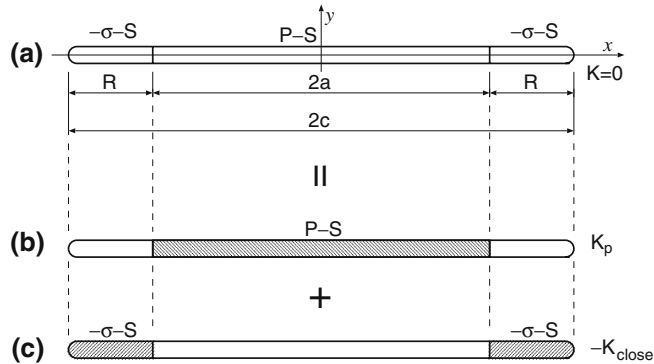


Figure 3

Problem analyzed by superimposing two subproblems with respect to applied pressure and cohesive stress: (a) original problem, (b) subproblem of applied pressure and (c) subproblem of cohesive stress.

It is assumed that the σ - δ relation is maintained under confined conditions as well as atmospheric (no confining pressure) condition. Therefore, K_c is the inherent material property and should be viewed as the fracture toughness of the rock.

This study analyzes the stress intensity factor required for crack growth when the fracture process zone is assumed to be negligibly small. This stress intensity factor corresponds to the apparent fracture toughness.

3. Theoretical Analysis

3.1. Stress Intensity Factor Based Analysis

This section presents the analytical results based on the stress intensity factor for both the cases of constant and linearly decreasing cohesive stress.

In order to derive a predictive model for the apparent fracture toughness, we considered subproblems with respect to the applied pressure and to the closing stress, as shown in Figure 3. The stresses acting on the crack in the problem to be analyzed, as shown in Figure 1, are the fluid pressure P , the cohesive stress σ and the confining stress S . The applied pressure that is the opening stress is the excess pressure ($P - S$) acting on the pressurized region $2a$. The closing stress is the composition of the cohesive stress and the confining stress ($-\sigma - S$) acting on the cohesive zone R .

The first subproblem is that of the crack, length $2c$, subjected to the applied pressure acting on the pressurized interval $2a$. The second subproblem is that of the crack subjected to the closing stress acting on the cohesive zone R . The original problem can be analyzed by superimposing the solution of the two subproblems. In the original problem, the stresses at the crack tip ($x = \pm c$) have to be finite. This

requires that the stress intensity factor at the crack tip equals to zero. Based on this condition, the apparent fracture toughness that is produced by the applied pressure can be determined.

When the length of the cohesive zone is sufficiently small in comparison to the crack length, the stress intensity factor K_P produced by the applied pressure (see Figure. 3b) is

$$K_P = \Delta P \sqrt{\pi c} = \Delta P \sqrt{\pi(a + R)} \tag{3}$$

$$= \Delta P \sqrt{\pi a} \left(1 - \frac{R}{2a} + \dots \right) \tag{4}$$

where $\Delta P = P - S$ is the excess pressure. For $R/a \ll 1$,

$$K_P = \Delta P \sqrt{\pi a}. \tag{5}$$

K_P corresponds to the apparent fracture toughness, as mentioned above.

Considering a constant cohesive stress σ_c acting over the length R at the tip of a semi-infinite crack, the stress intensity factor K_{close} produced by the closing stress (TADA *et al.*, 1973a) is

$$K_{close} = \sqrt{\frac{8}{\pi}} (\sigma_c + S) \sqrt{R}. \tag{6}$$

The condition that the stress at the tip of the cohesive zone has to be finite requires

$$K_P - K_{close} = 0. \tag{7}$$

Substituting equation (6) into equation (7) yields

$$R = \frac{\pi}{8} \left(\frac{K_P}{\sigma_c + S} \right)^2. \tag{8}$$

The crack opening displacement at $x = \pm a$ due to the excess pressure ΔP (TADA *et al.*, 1973a) is

$$\delta_P = \frac{2(1 - \nu)}{G} \Delta P \sqrt{c^2 - a^2} \tag{9}$$

$$= \frac{2(1 - \nu)}{G} \Delta P \sqrt{2aR} \left(1 - \frac{R}{4a} + \dots \right). \tag{10}$$

For $R/a \ll 1$,

$$\delta_P = \frac{2(1 - \nu)}{G} \Delta P \sqrt{2aR}, \tag{11}$$

where ν is Poisson's ratio and G is the shear modulus. For a semi-infinite crack, the crack opening displacement due to the closing stress at the edge of the cohesive zone is

$$\delta_{close} = \frac{2(1-\nu)}{G} \cdot \frac{2}{\pi} (\sigma_c + S)R. \quad (12)$$

The overall crack opening displacement at $x = \pm a$ is

$$\delta_{|\pm a} = \delta_P - \delta_{close}. \quad (13)$$

The crack growth takes place when the crack opening displacement at $x = \pm a$ reaches the critical crack opening displacement δ_c . Considering the crack growth condition, $\delta_{|\pm a}$ in equation (13) is replaced by δ_c . Then, substituting equations (1), (8), (11) and (12) into equation (13), yields

$$\frac{K_P^2}{K_c^2} = 1 + \frac{S}{\sigma_c}, \quad (14)$$

where $E' = E/(1-\nu)$ and $G = E/2(1+\nu)$ were used.

Equation (14) suggests that the stress intensity factor required for crack growth under confining pressure should exceed the inherent material property K_c due to the presence of the cohesive zone. Equation (14) provides a predictive model for the apparent fracture toughness when the cohesive stress is assumed to be constant.

Next, the case where the cohesive stress decreases linearly from the crack tip is considered.

In this case, in order to evaluate the stress intensity factor due to the cohesive stress, the distribution of cohesive stress along the crack should be given. However, the cohesive stress distribution is not linear since the crack opening displacement is not proportional to the distance from the crack tip. Therefore, the profile of crack opening displacement is needed for a rigorous analysis. Nonetheless, in this study, a linear distribution of cohesive stress along the crack is assumed for simplicity as

$$\sigma = \sigma_c \left(1 - \frac{\xi}{R}\right), \quad (0 \leq \xi \leq R), \quad (15)$$

where ξ is the distance from the crack tip. This approximation results in an error of about 10%, as described below. For this case, the stress intensity factor produced by the cohesive stress is obtained by integrating the stress intensity factor for the problem of the semi-infinite crack with a point load (TADA *et al.*, 1973b)

$$K_{close} = \frac{4}{3\pi} \sigma_c \sqrt{2\pi R}. \quad (16)$$

Therefore, the cohesive zone length is

$$R = \frac{\pi}{8} \frac{K_P^2}{\left(\frac{2}{3}\sigma_c + S\right)^2}, \quad (17)$$

where K_P is given by equation (5).

The crack opening displacement due to the cohesive stress is obtained by integrating the crack opening displacement for the semi-infinite crack with a point load (TADA *et al.*, 1973b)

$$\delta_{close} = \frac{2(1-\nu)}{G} \cdot \frac{2}{3\pi} \sigma_c R. \quad (18)$$

K_c is given by equation (2), then the result is

$$\frac{K_P^2}{K_c^2} = \frac{2\left(\frac{2}{3} + \frac{S}{\sigma_c}\right)^2}{1 + \frac{S}{\sigma_c}}. \quad (19)$$

Equation (19) indicates that K_P^2/K_c^2 becomes 8/9 when the confining pressure is zero ($S = 0$). This deviation from unity may be due to the approximation of the cohesive stress distribution along the crack.

3.2. Fracture Energy Based Analysis

This section describes an analysis based on the fracture energy concept. The fundamental idea is that the energy required for opening the crack under confining pressure is the sum of the two components needed to overcome the confining pressure as well as the cohesive stress.

When the cohesive zone length is small, for the constant cohesive stress case, the total fracture energy is

$$G_{total} = \sigma_c \delta_c + S \delta_c = \frac{K_P^2}{E'}. \quad (20)$$

When the confining pressure is zero, the total fracture energy is given by

$$G_{total} = \sigma_c \delta_c = \frac{K_c^2}{E'}. \quad (21)$$

Dividing (20) by (21), yields

$$\frac{K_P^2}{K_c^2} = 1 + \frac{S}{\sigma_c}. \quad (22)$$

This equation is in agreement with equation (14), which is derived based on the stress intensity factor. On the basis of the fracture energy approach, a solution for a general stress distribution (nonlinear) also can be obtained.

When the cohesive stress is provided by

$$\sigma = \sigma_c \left(1 - \frac{\delta}{\delta_c}\right)^n, \quad (23)$$

the fracture energy can be calculated for unconfined conditions by the J -integral

$$\frac{K_c^2}{E'} = \int_0^{\delta_c} \sigma d\delta = \frac{\sigma_c \delta_c}{n+1}. \quad (24)$$

Therefore, under the confining pressure, the total fracture energy is

$$\frac{K_P^2}{E'} = \frac{\sigma_c \delta_c}{n+1} + S \delta_c. \quad (25)$$

Then, the apparent fracture toughness can be obtained as

$$\frac{K_P^2}{K_c^2} = 1 + (n+1) \frac{S}{\sigma_c}. \quad (26)$$

When n is zero (constant cohesive stress), equation (26) coincides with equation (14). When n is unity, equation (26) corresponds to the linear decreasing cohesive stress case.

The predictive model of equation (26) holds true independent of the loading configuration. The only requirement is that the fracture process zone is small enough in comparison to the crack length.

Next, the result from the fracture energy approach is compared with that obtained based on the stress intensity factor. Thus, three equations (14), (19) and (26) deduced in this study are compared in Figure. 4. In this figure, equation (26) with $n = 1$ is compared with equation (19). The increasing tendency of equation (26) is consistent with equation (19), although equation (19) shows slightly smaller values due to the

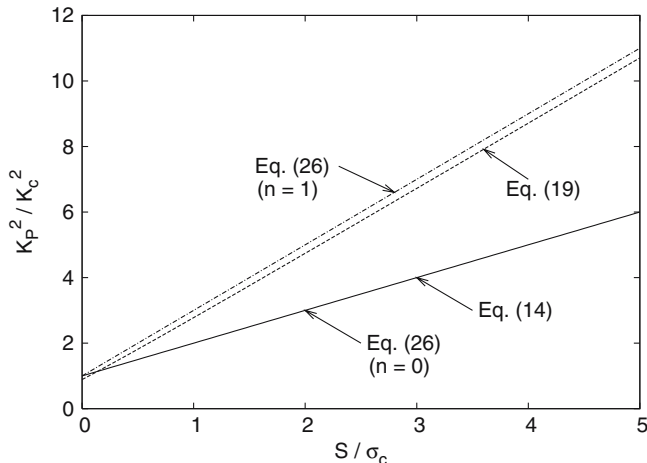


Figure 4

Comparison of derived equations. Equation (14) and equation (26) with $n = 0$ corresponds to the case of the constant cohesive stress. equation (19) and equation (26) with $n = 1$ corresponds to the case of the linear cohesive stress.

approximation of the stress distribution along the crack. The formulation obtained from the fracture energy approach is expected to provide a general model for predicting the increase of the apparent fracture toughness under confining pressure.

The apparent fracture toughness significantly increases with the confining pressure. This result demonstrates that the fracture toughness increases when the fracture process zone exists at the crack tip, even if the size of the fracture process zone is negligibly small.

4. Numerical Analysis

4.1. Numerical Procedure

In order to examine the validity of the derived equations, numerical analyses were performed in this study.

Two-dimensional numerical computations were also carried out, based on the cohesive crack model, in addition to the theoretical analysis described in the previous sections. The body force method (NISHITANI, 1968; NISHITANI *et al.*, 1990) was used to determine the stress intensity factor and the inner pressure. The body force method allows us to examine the effect of confining pressure on the apparent fracture toughness, under the condition in which the extent of the cohesive zone is not negligibly small. The problem configuration is shown in Figure. 1. In the numerical computations, the size of the cohesive zone and the cohesive stress were predetermined and the inner pressure was adjusted to maintain the stress intensity factor zero at the crack tip ($x = \pm c$). Therefore, the fracture toughness K_c was varied by changing the size of the cohesive zone and cohesive stress in the computations. Here, K_c is evaluated by equations (1) or (2). The size parameter of the cohesive zone, R/c in the numerical computations was in the range of $0.001 \cong 0.5$. As seen in the size parameter, the numerical computations were conducted to include the condition in which the size of the cohesive zone is nonnegligible with respect to the crack length.

4.2. Numerical Results and Discussion

Figures 5 and 6 show the dependency of K_c on the cohesive zone size obtained by numerical calculations. Figure 5 is obtained for the constant cohesive stress condition and Figure. 6 is for the linearly decreasing stress condition. The fracture toughness K_c increases with the increase of the cohesive zone size. For the same cohesive zone length, K_c increases with increasing confining pressure.

The numerical results are compared with the analytical solutions. The dependency of apparent fracture toughness on the confining pressure is shown in Figures. 7(b) and 8(b), for the constant cohesive stress condition and for the linearly decreasing stress condition, respectively. These figures were constructed by selecting

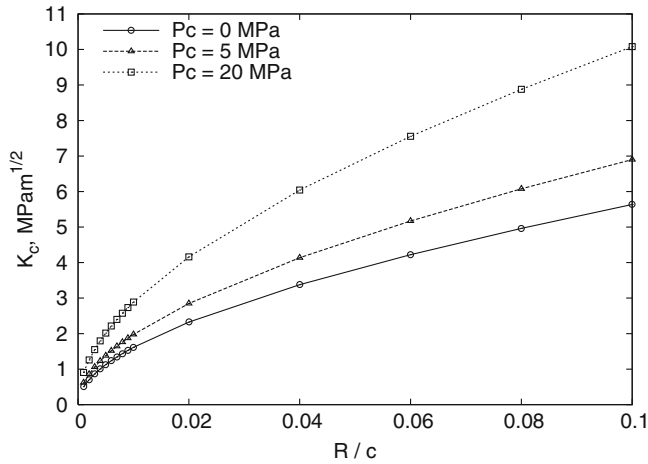


Figure 5

Dependency of K_c on the cohesive zone size R for the case of constant cohesive stress.

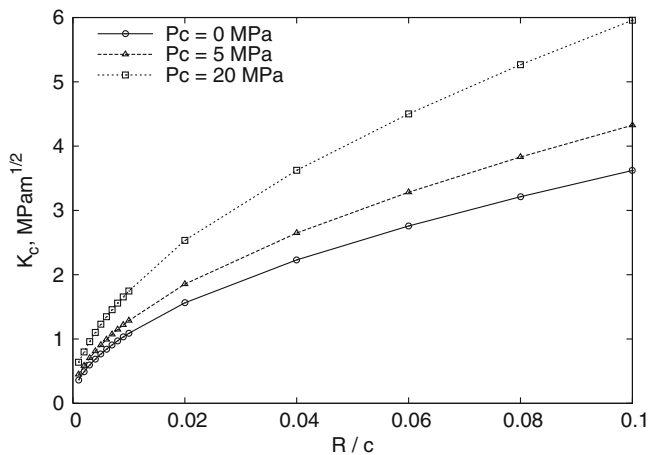


Figure 6

Dependency of K_c on the cohesive zone size R for the case of linear cohesive stress.

the set of data presented in Figures. 5 and 6 which provided the similar same K_c value. The analytical results given by equations (14) and (26) are indicated as solid lines in Figures. 7(b) and 8(b), respectively. In the case of the linearly decreasing cohesive stress, the parameter n in equation (26) is taken to be 1.0. The apparent fracture toughness K_P is evaluated by equation (5).

Figures 7(a) and 8(a) show the cohesive zone size for different K_c values and confining pressure conditions. It can be seen that the numerical result obtained for the lower K_c value and smaller R/c is very close to the trend predicted by the

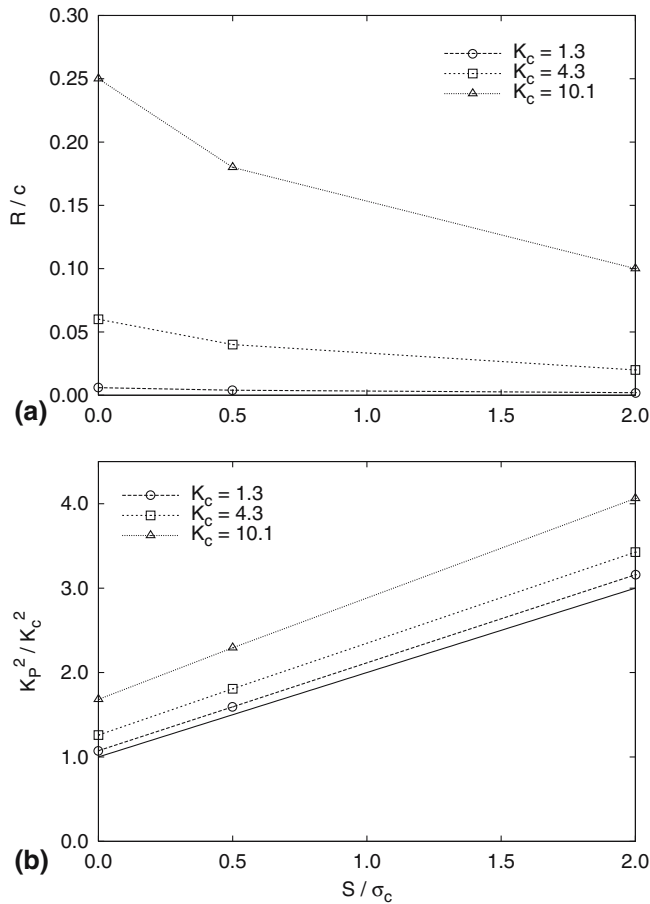


Figure 7

Comparison of numerical results and the analytical solution for the case of constant cohesive stress: (a) Size of cohesive zone and (b) dependency of apparent fracture toughness on confining pressure.

theoretical analysis. This evidence demonstrates the validity of the theoretical analysis for the condition of the negligible cohesive zone size. When the K_c value increases and the cohesive zone size becomes larger with respect to the crack length, the numerical result tends to deviate from the theoretical result. It is very interesting to note that the slope in the plot of $K_p^2/K_c^2 - S/\sigma_c$ shows no drastic change even when the cohesive zone size becomes larger.

The apparent fracture toughness significantly increases with increasing confining pressure as shown in Figs. 7 and 8. MATSUKI *et al.* (1995) have stated that the reason for the increase of apparent fracture toughness is the closure of pre-existing cracks involved in the rock specimen. This causes the rock specimen to become less damaged material. RUBIN (1993), and FIALKO and RUBIN (1997) have reported that

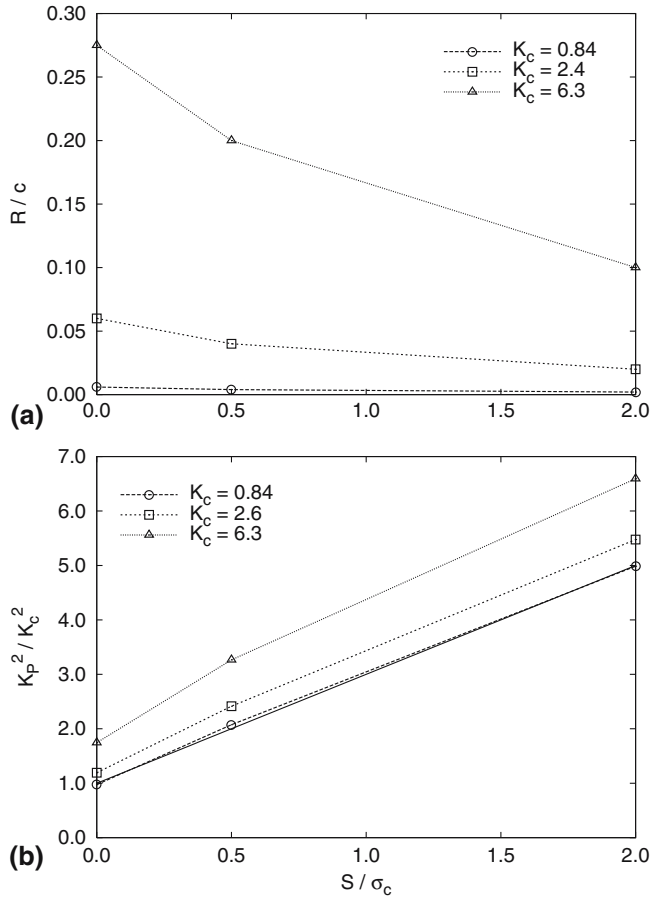


Figure 8

Comparison of numerical results and the analytical solution for the case of linear cohesive stress: (a) Size of cohesive zone and (b) dependency of apparent fracture toughness on confining pressure.

the high tensile stress field appears off crack plane when the confining pressure becomes sufficiently high. The magnitude of the tensile stress can be higher than the peak cohesive stress, namely the tensile strength of rocks. They have concluded that the increase of the apparent fracture toughness is the result of inelastic deformation near the crack tip region due to this high tensile stress. However, no quantitative model has been proposed for predicting the increase of apparent fracture toughness under higher confining pressures. In contrast with the above-mentioned previous studies, the present study points out the different mechanism for the increase of apparent fracture toughness. Based on our theoretical analysis, we propose that the apparent toughness increase may be due to the additional energy required to open up the crack flank within the cohesive zone against the confining pressure. Furthermore,

a quantitative model for the apparent toughness increase has been derived based on the theoretical analysis.

5. Concluding Remarks

The present study provides a predictive model for the apparent fracture toughness, which was derived on the basis of a cohesive crack model. A two-dimensional fluid-driven fracture with a cohesive zone under confining pressure was analyzed. Two types of cohesive stress distributions were studied. Furthermore, the problem for more general cohesive stress distribution was analyzed based on the fracture energy concept. The size of the cohesive zone was assumed to be negligibly small. The apparent fracture toughness was measured as the stress intensity factor induced by the fluid pressure. The derived results were compared with numerical results.

The analytical solution suggests a substantial increase in the apparent fracture toughness due to the increased confining pressures, even if the size of the fracture process zone is small. The apparent fracture toughness is shown to be a function of the tensile strength (the peak value of the cohesive stress) and confining pressure. Their functional form depends on the cohesive stress distribution. Consequently, the evaluation of the fracture process zone in rocks is of importance to fracture problems.

REFERENCES

- ABOU-SAYED, A.S. (1978), *An experimental technique for measuring the fracture toughness of rock under downhole stress condition*, VDI-Berichte 313, 819–824.
- FIALCO, Y.A. and RUBIN, A.M., (1997), *Numerical simulation of high-pressure rock tensile fracture experiments: Evidence of an increase in fracture energy with pressure?* Int. J. of Geophys. Res. 102-B3, 5231–5242.
- FUNATSU, T., SETO, T., SHIMADA, H., MATSUI, K. and KURUPPU, M. (2004), *Combined effects of increasing temperature and confining pressure on the fracture toughness of clay bearing rocks*, Int. J. of Rock. Mech. and Min. Sci. 41, 927–938.
- HASHIDA, T. *Evaluation of fracture processes in granites based on the tension-softening model*. In *Micromechanics of Failure of Quasi-Brittle Materials* (eds. Mihashi, H., Takahashi, H. and Wittmann, F. H.) (Elsevier Applied Science, 1990) pp. 233–243.
- HASHIDA, T., OGHIKUBO, H., TAKAHASHI, H. and SHOJI, T. (1993), *Numerical simulation with experimental verification of the fracture behavior in granite under confining pressures based on the tension-softening model*, Int. J. of Fracture 59, 227–244.
- HILLERBORG, A. *Analysis of one single crack*, In *Fracture Mechanics of Concrete* (ed. Wittmann F.H.) (Elsevier Science Publishers B. V., Amsterdam, 1983) pp. 223–250.
- LABUZ, J. F., SHAH, S. P. and DOWDING, C. H. (1987), *The fracture process zone in granite: Evidence and effect*, Int. J. Rock. Mech. Min. Sci. and Geomech. Abstr. 24–4, 235–246.
- MATSUKI, K., KANEKO, T. and SATO, T. (1995), *K-resistance curve of rock under confining pressure*, Shigen-to-Sozai (in Japanese) 111, 755–760.

- NISHITANI, H. (1968), *The two-dimensional stress problem solved using an electronic digital computer*, Bull. Japan Soc. Mech. Engrs. 11-43, 15–23.
- NISHITANI, H., SAIMOTO, A. and NOGUCHI, H. (1990), *Versatile method of analysis of two-dimensional elastic problem by body force method* (1st Report, Basic Theory), Trans. JSME(A) (in Japanese) 56-530, 2123–2129.
- RUBIN, A.M. (1993), *Tensile fracture of rock at high confining pressure: Implications for dike propagation*, Int. J. of Geophys. Res. 98-B9, 15, 919–15, 935.
- SATO, K., HASHIDA, T. and TAKAHASHI, H. *Acoustic emission study of process zone in granite and tension-softening model*. In *AE/MS Activity in Geological Structures and Materials* (ed. Hardy, JR., H.R.) (Trans Tech Publications, 1995) pp. 81–95
- SCHMIDT, R.A. and HUDDLE, C.W. (1977), *Effect of confining pressure on fracture toughness of Indiana limestone*, Int. J. Rock. Mech. Min. Sci. and Geomech. Abstr. 14, 289–293.
- TADA, H, PARIS, P.C., and IRWIN, G.R. (1973a), *The Stress Analysis of Cracks Handbook*, Del Research Corporation, 3.7
- TADA, H, PARIS, P.C., and IRWIN, G.R. (1973b), *The Stress Analysis of Cracks Handbook*, Del Research Corporation, 3.6

(Received February 28, 2005, revised October 28, 2005, accepted November 4, 2005)

Published Online First: May 12, 2006



To access this journal online:
<http://www.birkhauser.ch>
